Stability and speedup issues in TTI RTM implementation

Kwangjin Yoon, Sang Suh, Jean Ji, James Cai, and Bin Wang, TGS

Summary

In the implementation of TTI RTM, we meet stability problems and demands for speedup. Staggered Fourier first derivative and linear interpolation improves stability and accuracy. Areas with high gradients of the symmetry axis give rise to unstable numerical computations and make the wavefield blow up. Selective matching of anisotropy parameters helps to eliminate these areas. The acoustic TTI wave equation needs intensive computing. The finite difference method is more flexible than pseudo-spectral method. However, the pseudo-spectral method gives a more accurate solution than the finite difference method. Efficiency can be improved by combining pseudo-spectral and finite difference methods.

Introduction

Subsurface geologic properties are very complex. To obtain the correct subsurface seismic image, we need to 1) estimate accurate parameters, such as velocity, epsilon, delta, dip and azimuth, and 2) use migration algorithms which express wave phenomena properly in the media. In reverse time migration (RTM) (Baysal et al, 1983; Whitmore, 1983), the accuracy of the migrated image depends on how well the migration algorithm simulates real seismic wave propagation. Because most rocks have anisotropy and sediments have layer induced anisotropy (Thomsen, 1986), RTM needs to take anisotropy into account to obtain correct images.

Alkhalifah (2000) derived a vertically transverse isotropic (VTI) acoustic wave equation by assuming zero shear wave vertical velocity and this equation provided an easy way to implement anisotropic RTM. Alkhalifah's fourth-order VTI acoustic wave equation reduces computational cost and simulates *P*-wave propagation without separation of *P* and *S* waves. Zhou et al. (2006a) modified Alkhalifah's fourth-order equation to a second-order equation, which is easy to implement using the finite difference method. Based on the Alkhalifah's approximation of zero shear wave vertical velocity, second-order tilted transverse isotropic (TTI) acoustic wave equations have been introduced (Zhou et al., 2006b; Fletcher et al., 2009).

Figure 1 shows the benefit of TTI RTM. Figure 1(a) and 1(b) are 3D VTI and TTI RTM images, respectively, in Gulf of Mexico. The parameters including velocities are estimated independently in VTI and TTI media and then final RTMs have been run. TTI RTM gives better quality especially in deep steeply dipping events and subsalt areas. This comparison demonstrates that the process based on TTI media produces a better image than that on VTI media.

TTI acoustic wave equations include second derivatives, coupled first derivatives and coefficients of dip or azimuth. Numerical computation of the coupled first derivative demands more computations and accurate implementation to avoid unstable or erroneous wave propagation. The pseudo spectral method (PSM) has the accuracy to calculate derivatives with about two grid points per wavelength (Kosloff et al., 1982; Fornberg, 1987). The finite difference method (FDM) is less accurate but more flexible than the pseudo-spectral method especially for domain decomposition. The FDM can get a solution faster than PSM for the same number of grid points. However, both are comparable considering the highest frequency they can handle. Efficiency can be improved by combining PSM and FDM.

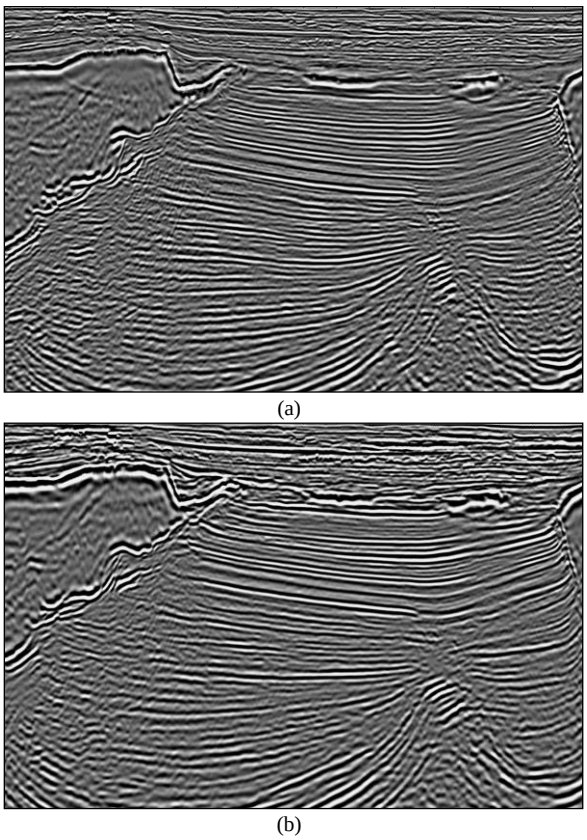

(a)

(b)

Figure 1. (a) VTI and (b) TTI RTM images in Gulf of Mexico.

Stability issue in acoustic TTI RTM

A TTI acoustic wave equation based on the Alkhalifah's zero shear wave vertical velocity is given as (Zhou et al., 2006b; Fletcher et al., 2009).

$$\frac{1}{v}\frac{\partial^2 p}{\partial t^2} = [(1+2\delta)H_2(p+q)+H_1 p]$$
$$\frac{1}{v}\frac{\partial^2 q}{\partial t^2} = [2(\varepsilon-\delta)H_2(p+q)]$$
$$H_1 = \sin^2\theta\cos^2\phi\frac{\partial^2}{\partial x^2}+\sin^2\theta\sin^2\phi\frac{\partial^2}{\partial y^2}+\cos^2\theta\frac{\partial^2}{\partial z^2}$$
$$+\sin^2\theta\sin 2\phi\frac{\partial^2}{\partial x\partial y}+\sin 2\theta\sin\phi\frac{\partial^2}{\partial y\partial z}+\sin 2\theta\cos\phi\frac{\partial^2}{\partial x\partial z}$$
$$H_2 = \frac{\partial^2}{\partial x^2}+\frac{\partial^2}{\partial y^2}+\frac{\partial^2}{\partial z^2}-H_1 \quad (1)$$

, where θ and φ are dip and azimuth. Anisotropic acoustic wave equations derived from the approximation of zero shear wave vertical velocity produce diamond-shape artifacts, SV-waves, propagating from the source point (Grechka et al., 2004). Figure 2 shows these artifacts in the impulse response using equation (1) in the TTI medium specified by P-wave velocity vertical to the symmetric plane $V_p = 2000m/sec$, dip $\theta = 45°$ and Thomsen anisotropic coefficients $\varepsilon = 0.24$, $\delta = 0.1$. These artifacts arise due to the anisotropy at the source point and are easy to remove by setting $\varepsilon = \delta$ around the source point (Duveneck et al., 2008).

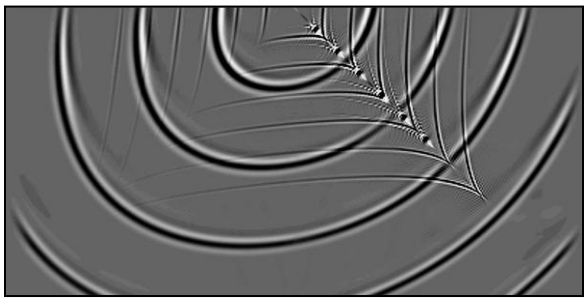

Figure 2. Impulse response using the TTI wave equation (1) and TTI medium $\varepsilon = 0.24$, $\delta = 0.1$, $\theta = 45°$ and $V_p = 2000m/sec$.

During the numerical computation of wave propagation using equation (1), areas with high anisotropic parameter gradients give rise to unstable numerical computations that cause the wavefield to blow up. Dip θ and azimuth φ, which are coefficients of derivative terms, are dominant sources of instability. Figure 3 shows a test of TTI RTM using BP TTI synthetic data and equation (1). Figure 3(a) is the dip of the model. Figure 3(b) and 3(c) are a forward modeling snapshot and RTM image which are contaminated with wavefield blow-up due to unstable computation.

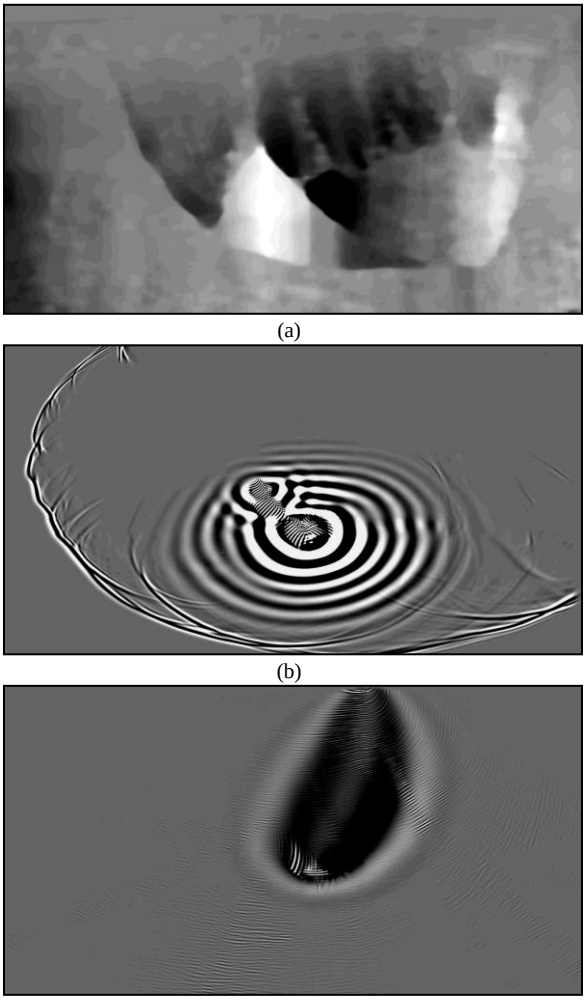

(a) (b) (c)

Figure 3. (a) dip of BP TTI synthetic model, unstable (b) a forward modeling snapshot and (c) RTM image.

To obtain a more correct RTM image, we need a stable and accurate wave propagator. Staggered grid computation of first derivatives in equation (1) helps to improve accuracy and stability. In PSM, staggered first derivative can be computed using the phase shift theorem (Correa et al., 2002). The phase shift operator for half grid spacing is $S^{\pm}(k) = e^{\mp ik\Delta x/2}$, where Δx is the grid spacing and k is the angular wavenumber $k = 2\pi j/(N\Delta x), j = 0, \ldots, N-1$ (Bracewell, 1986). The staggered grid first derivative in k domain is given as

$$U(k)|_{\Delta x/2} = U(k)e^{-i\Delta x/2} \quad (2)$$

, where $U(k)$ is the wavefield at normal, or centered, grids in the k domain, which is defined by $U(k) = DFT\{u(x)\}$. Correa et al. (2002) showed that staggered odd-order and centered even-order Fourier derivatives are compact. For accurate implementation of the TTI acoustic wave equation (1), first and second derivatives are to be computed at staggered and centered grids, respectively. For the wavefield update to the next time step in equation (1), $U(k)|_{\Delta x/2}$ can be interpolated into centered grids using FFT interpolation before or linear interpolation after the transform to the space domain. The impulse response in Figure 2 has been produced using the FFT interpolation in the wave number domain. FFT interpolation gives the exact solution for a periodic function. Clear diamond-shape artifacts in the impulse response demonstrate the accuracy of FFT interpolation.

On the other hand, Figure 4 shows the TTI RTM image using linear interpolation after transform to the space domain. The artifacts in Figure 4 do not form clear diamond-shapes, which means that the linear interpolation is not as accurate as the FFT interpolation. Both impulse responses in Figure 2 and Figure 4 look very similar except the artifacts. Acoustic TTI RTM using FFT interpolation is accurate but not stable in heterogeneous media. Linear interpolation is less accurate but more stable than FFT interpolation in implementation of TTI RTM using equation (1).

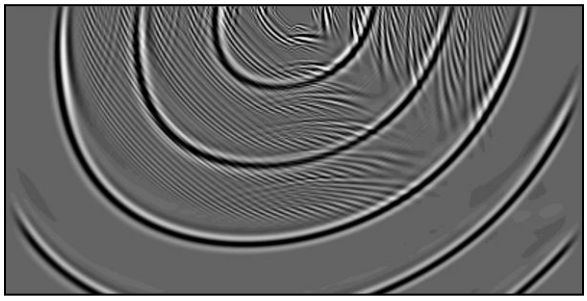

Figure 4. Impulse response using the TTI wave equation (1) with parameters of $\varepsilon = 0.24$, $\delta = 0.1$, $\theta = 45°$ and $V_p = 2000m/sec$. This TTI RTM image has been produced by linear interpolation after transform to space domain.

Staggered grid first derivative and linear interpolation of the first derivative to normal grids improves accuracy and stability. These techniques provide stable wavefields in areas of mild variation in the symmetry axis. However, some spots of high symmetry axis gradient produce large instabilities, which cannot be handled with these techniques, and make wavefields blow up. Symmetric axis change brings about the unstable wavefield, but the instability is originated by anisotropy. In regions where wavefield instability can occur, the anisotropy can be taken off by following the method which sets $\varepsilon = \delta$ to suppress artifacts from the source point in an anisotropic medium. SV wavefront triplication can be suppressed by using small $\sigma = V_{pz}/V_{sz}(\varepsilon - \delta)$, where V_{pz} and V_{sz} are the P and S wave velocities along the symmetry axis (Tsvankin, 2001; Fletcher et al., 2009). Instead of large V_{sz}, we can make $\varepsilon = \delta$ around the spots of high symmetry axis gradient. Figure 5 is the plot of weighting coefficients determined by the gradient of the dip shown in Figure 3(a) for the selective anisotropic parameter matching. A weighting coefficient at a grid point is set to 1 if the symmetry axis gradient exceeds some threshold, otherwise it is 0. The threshold has been chosen empirically.

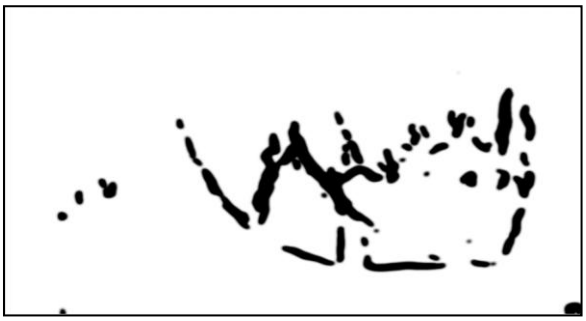

Figure 5. Plot of weighting coefficients for selective anisotropic parameter matching. A coefficient becomes 1, black color, if the gradient of symmetry axis exceeds the empirically determined threshold.

Figure 6 shows stable (a) a forward modeling snapshot and RTM images (b) of one shot gather and (c) all shot gathers. TTI RTM has been implemented using the staggered grid first derivative plus linear interpolation and the selective anisotropic matching techniques. Figure 7 is the TTI RTM image of the BP TTI synthetic dataset.

Speed up issue in acoustic TTI RTM

TTI acoustic wave equation in equation (1) demands intensive computation, more than five or six times the isotropic wave equation. High order FDM or PSM can reduce memory and computational cost with coarse grid spacing. FDM is more flexible than PSM. FDM can restrict computations within the zone between the first arriving wave fronts and the source point. FDM is easier than PSM to apply domain decomposition. However, PSM has the benefit that it can handle higher frequency than FDM at the same grid spacing. Empirically speaking, PSM can get an accurate numerical solution of the acoustic wave equation having V_p parameter only with about 2.3 grid points per wave length under the 4th order time integration scheme (Dablain, 1986). But high order FDM (Dablain, 1986; Holberg, 1987) needs more than 2.6 grid points for an accurate solution.

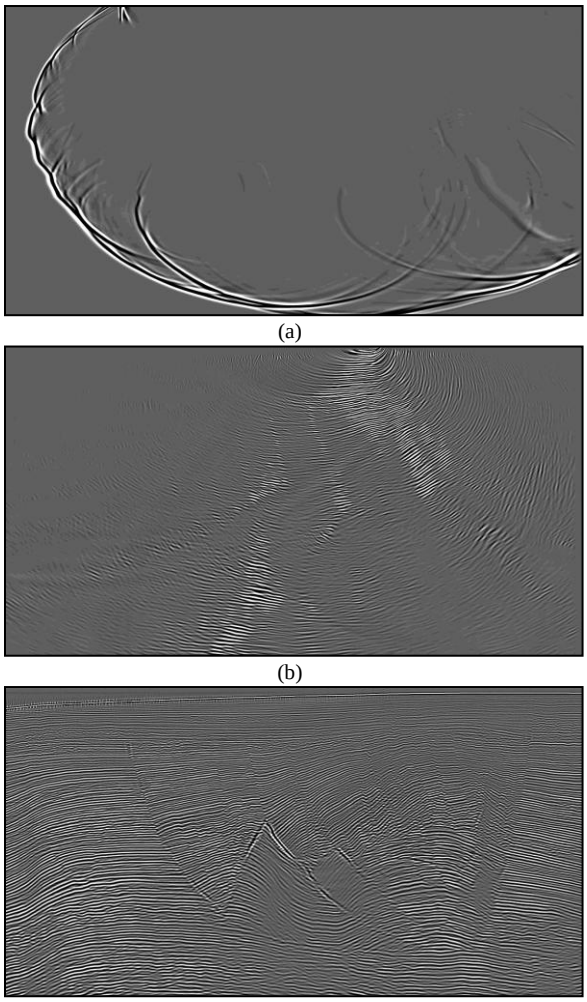

Figure 6. Stable (a) a forward modeling snapshot and TTI RTM images using (b) one shot and (c) all shots of BPTTI data.

In FDM, performance increases with the order of stencil up to about the 16th order. However, the performance of PSM depends on the FFT library. The CPU time of FFT is not linearly related to the length of FFT. To achieve the best performance, the FFT length has to be determined by scanning the CPU times of various FFT lengths. For a fixed size of volume, 3D FFT or 2D FFT are faster than 1D FFT. However, considering the nonlinear FFT performance and implementation efficiency, 1D FFT is more flexible and gives better performance than 2D or 3D FFTs.

Subsurface velocity usually increases with depth and the grid spacing is determined by the minimum velocity and highest frequency. In case the fixed grid spacing is applied, PSM is suitable for low velocity areas and FDM can be applied to higher velocity areas. By combining PSM and high order FDM, we can further reduce the memory and CPU time.

Conclusions

The TTI acoustic wave equation is more unstable and expensive to solve than VTI or isotropic wave equations. Staggered grid first derivative plus linear interpolation improves accuracy and stability in the numerical solution. Areas of high symmetry axis gradient generating unstable wavefields can be erased by selective anisotropic parameter matching. High order FDM and PSM can speed up TTI RTM. The performance of TTI RTM can be further improved by combining FDM and PSM.

Acknowledgments

The authors thank BP for the synthetic data set and TGS management for permission to publish this paper. We thank Simon Baldock, Laurie Geiger and Shannon Morelez in TGS for their reviews.

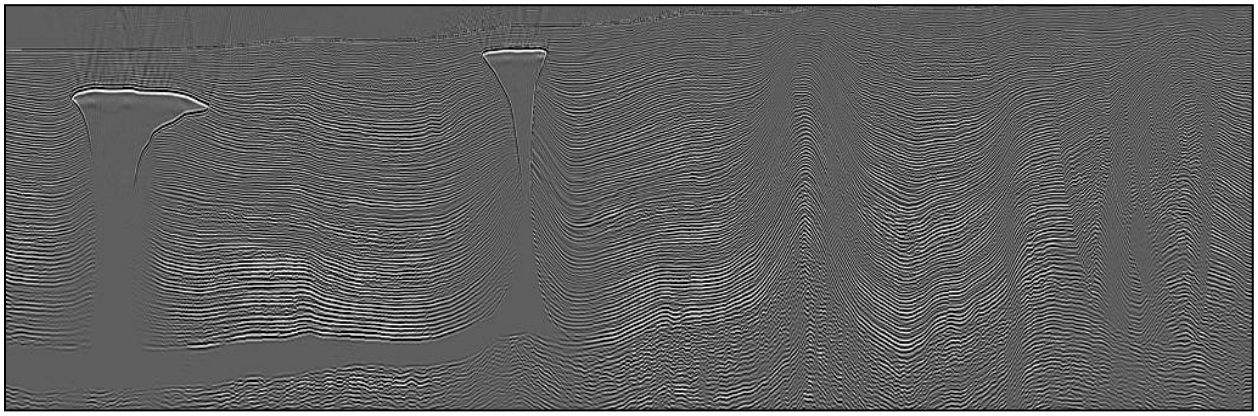

Figure 7. TTI RTM image of BPTTI synthetic data.

EDITED REFERENCES

Note: This reference list is a copy-edited version of the reference list submitted by the author. Reference lists for the 2010 SEG Technical Program Expanded Abstracts have been copy edited so that references provided with the online metadata for each paper will achieve a high degree of linking to cited sources that appear on the Web.

REFERENCES

Alkhalifah, 2000, An acoustic wave equation for anisotropic media: Geophysics, **65**, 1239-1250.

Baysal, E., D. D. Kosloff, and J. W. C. Sherwood, 1983, Reverse-time migration: Geophysics, **48**, 1514–1524, doi:10.1190/1.1441434.

Bracewell, R., 1986, The Fourier transform and its applications: McGraw-Hill.

Correa, G., M. Spiegelman, and S. Carbotte, 2002, Centered and staggered Fourier derivatives and Hilbert transforms: Geophysics, **67**, 1558–1563. doi:10.1190/1.1512801

Dablain, M. A., 1986, The application of high-order differencing to the scalar wave equation: Geophysics, **51**, 54–66, doi:10.1190/1.1442040.

Duveneck, E., P. Milcik, P. M. Bakker, and C. Perkins, 2008, Acoustic VTI wave equation and their application for anisotropic reverse-time migration: 78th Annual International meeting, SEG, Expanded Abstracts, 2186-2190.

Fletcher, R., X. Du, and P. J. Fowler, 2009, Reverse time migration in TTI media: Geophysics, **74**, no. 6, WCA179–WCA187. doi:10.1190/1.3269902

Fornberg, B., 1987, The pseudospectral method: Comparisons with finite differences for the elastic wave equation: Geophysics, **52**, 483–501, doi:10.1190/1.1442319.

Grechka, V., L. Zhang, and J. W. Rector III, 2004, Shear waves in acoustic anisotropic media: Geophysics, **69**, 576–582, doi:10.1190/1.1707077.

Holberg, O., 1987, Computational aspects of the choice of operator and sampling integral for numerical differentiation in large-scale simulation of wave phenomena: Geophysical Prospecting, **35**, no. 6, 629–655, doi:10.1111/j.1365-2478.1987.tb00841.x.

Kosloff, D. D., and E. Baysal, 1982, Forward modeling by a Fourier method: Geophysics, **47**, 1402–1412, doi:10.1190/1.1441288.

Thomsen, L., 1986, Weak elastic anisotropy: Geophysics, **51**, 1954–1996, doi:10.1190/1.1442051.

Tsvankin, I., 2001, Seismic signatures and analysis of reflection data in an isotropic media: Elsevier.

Whitemore, N. D., 1983, Iterative depth imaging by backward time propagation: 53rd Annual International Meeting, SEG, Expanded Abstracts, 382-385.

Zhou, H., G. Zhang, and R. Bloor, 2006a, An anisotropic acoustic wave equation for VTI media: 68th Annual conference and Exhibition, EAGE, Extended Abstracts, H033

Zhou, H., G. Zhang, and R. Bloor, 2006b, An anisotropic acoustic wave equation for modeling and migration in 2D TTI media: 76th Annual International meeting, SEG, Expanded Abstracts, 194-198.